Acta Polytechnica CTU Proceedings **36**:175–184, 2022
https://doi.org/10.14311/APP.2022.36.0175

Published by the Czech Technical University in Prague

STATISTICAL CHARACTERISATION OF REINFORCEMENT PROPERTIES FOR TEXTILE-REINFORCED CONCRETE: A NOVEL APPROACH

Marcus Ricker[a], Sergej Rempel[b], Tânia Feiri[a,*], Jan Schulze-Ardey[c], Josef Hegger[c]

[a] *Hochschule Biberach University of Applied Sciences, Institute of Structural Engineering, Karlstraße 11, 88400 Biberach, Germany*

[b] *Hochschule Augsburg University of Applied Sciences, Faculty of Architecture and Civil Engineering, An d. Hochschule 1, 86161 Augsburg, Germany*

[c] *RWTH Aachen University, Institute of Structural Concrete, Mies-van-der-Rohe-Str. 1, 52074 Aachen, Germany*

[*] corresponding author: feiri@hochschule-bc.de

Abstract. The potential of textile-reinforced concrete is broad: it can be used in new structures and in the retrofitting of existing structural components. Designing textile-reinforced concrete requires knowledge about the mechanical properties of different textile types. To this, a standardised tensile test for fibre strands was used. The test aims to statistically characterise two material properties needed in design: ultimate tensile strength and the modulus of elasticity. To this, the influence of length and number of fibre strands were evaluated. The results show that the ultimate tensile strength can be statistically modelled by a Gumbel distribution and the modulus of elasticity can be characterised by a Normal distribution. These findings can be used to derive appropriate partial safety factors for the design value of tensile strength using probabilistic methods, or to directly determine the failure probability of textile-reinforced concrete components.

Keywords: AR-glass reinforcement, carbon concrete, carbon reinforcement, design provisions, standardised tensile test for fibre strands, textile-reinforced concrete.

1. Introduction

Textile-reinforced concrete (TRC) is a composite construction material that combines the use of a matrix of fine-grained concrete and mesh-like fibre reinforcements made of alkali-resistant (AR) glass, polymeric, carbon or basalt, among others. As it has been largely demonstrated by the scientific community and practitioners, the construction sector has been showing a growing interested is the use of TRC in structures. This is mostly due to favourable mechanical properties of TRC, namely the high tensile strength and durability [1–9]. In fact, the range of potential civil engineering applications is not exclusive to new structures, as the carbon concrete bridge in Ebingen (Germany) [10]; TRC is also a prime alternative to retrofit and rehabilitate reinforced concrete structures.

Yet, the acceptance and utilisation of TRC structural solutions depend on the availability of clear design guidelines, installation procedures and construction specifications. To overcome the lack of clear design guidelines, normally, building authorities request proofs of usability [13] by means of individual approvals (e.g., a "ZiE" in Germany) or even general permits (e.g., European Technical Assessments). Consequently, load-bearing tests are needed to evaluate the ultimate and the serviceability limit states, which can be complex, costly and also slow [3, 12, 14]. Thus, there is little doubt that alternative design approaches that do not depend on exhaustive experimental campaigns would be valuable to the structural design community.

Previous investigations have showed that as opposed to steel reinforcement, AR-glass or carbon reinforcement has a linear-elastic behaviour without a pronounced yield plateau and such reinforcement can have three to seven times higher ultimate tensile strengths [3, 12]. These properties have motivated Hinzen [11] to propose a standardised tensile test for fibre strands. This standardised tensile test can support the derivation of design values of textile reinforcement (e.g., epoxy resin-soaked AR-glass reinforcement) and has the benefit to consider the impact of the weaving structure on the material parameters of fibre strands, namely damages and distortions during weaving. This means that the material properties of individual fibres are not necessarily needed for the reinforcement design [15].

In the context of this investigation, two relevant textile reinforcement properties were considered – (1) ultimate tensile strength and (2) modulus of elasticity – whose statistical parameters can be determined through the standard tensile test. The statistical characterisation of these properties is vital for the assessment of failure probabilities of textile-reinforced concrete members and/or for the calculation of partial safety factors. As numerous scientific

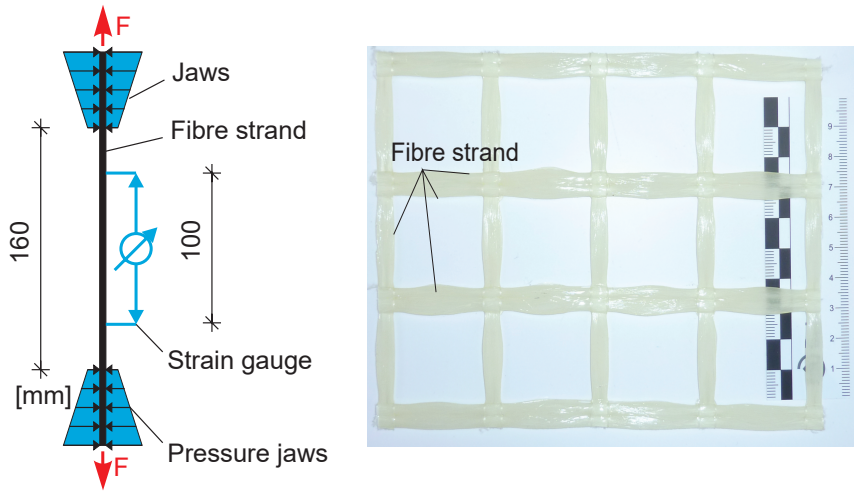

Figure 1. (a) Standardised tensile test [11]. (b) Testing grid of AR-glass reinforcement [12].

studies demonstrate (e.g., [16–18]), probability-based concepts are used during safety level evaluations of structural components. Thus, there is little doubt that a probabilistic-based reasoning is essential to derive new design provisions and/or to improve existing ones.

In this investigation, the results of a standardised tensile test on an epoxy resin-soaked AR-glass textile are adopted for the calculation of statistical parameters of ultimate tensile strength and modulus of elasticity. Nonetheless, a similar approach can be adopted for all epoxy resin-soaked fibre strands. For the sake of this investigation, it should be made clear that multiple fibres form a filament and multiple filaments compose a strand [19]. Finally, it is also relevant to mention that the results of the experimental campaign presented in this investigation were partially discussed in another publication [20].

2. Description of the standardised tensile test

2.1. Characterisation of the test setup

The standardised tensile test proposed by Hinzen [11] was used to determine the behaviour of a textile reinforcement (e.g., AR-glass textiles soaked with epoxy resin). Individual fibre strands with the lengths of 60 mm, 160 mm, 320 mm, and 640 mm were cut out of the soaked and cured textile. These were used to investigate the influence of the fibre strand length. Further, a tension load was directly applied on a reinforced concrete body through pressure jaws to guarantee that the strands were evenly loaded. The strain was registered with two clamp-on strain transducers over a length of 100 mm (Figure 1). The strain was also recorded with linear variable differential transformers (LVDTs) over a reference length of 450 mm. This experimental setup followed the RILEM recommendations [21]. Seven tensile test series were conducted on composite members reinforced with different number of fibre strands.

2.2. Characterisation of the material parameters

The results of the standardised tensile tests are shown in the stress-strain diagram in Figure 2a. An idealised stress-strain relationship is derived from the measurements, which can be later used for the cross-sectional design of a component. The textile stress σ_t is calculated from the measured force F and the accumulated fibre strands cross sectional area A_r (Equations 1).

By using the results of the standardised tensile test, the material behaviour of the fibre strands with a linear-elastic approach can be determined with Equations 1 and 2. The parameters are: (i) the mean value of the modulus of elasticity (or Young's modulus) E_{tm}, (ii) the ultimate tensile strength $f_{t,u}$, and (iii) the ultimate strain $\varepsilon_{t,u}$. In principle, only two of the parameters are required for the characterisation of the textile reinforcement:

$$\sigma_t = \frac{F}{A_r} = \varepsilon_t \cdot E_{tm} \leq f_{t,u} \tag{1}$$

$$\varepsilon_t = \frac{\sigma_t}{E_{tm}} \leq \varepsilon_{t,u} \tag{2}$$

By assuming a linear-elastic behaviour, the textile stress value of each strain (Equation 1) and the strain value of each stress (Equations 2) can be determined for each point of the stress-strain diagram by using the mean value of the modulus of elasticity. The relationship between these parameters is illustrated in Figure 2b. Equations 2a and 2b guide the design approach represented in Figure 2a.

2.3. Results of the experimental campaign

In this experimental campaign, more than 400 standardised tensile tests were conducted to describe the

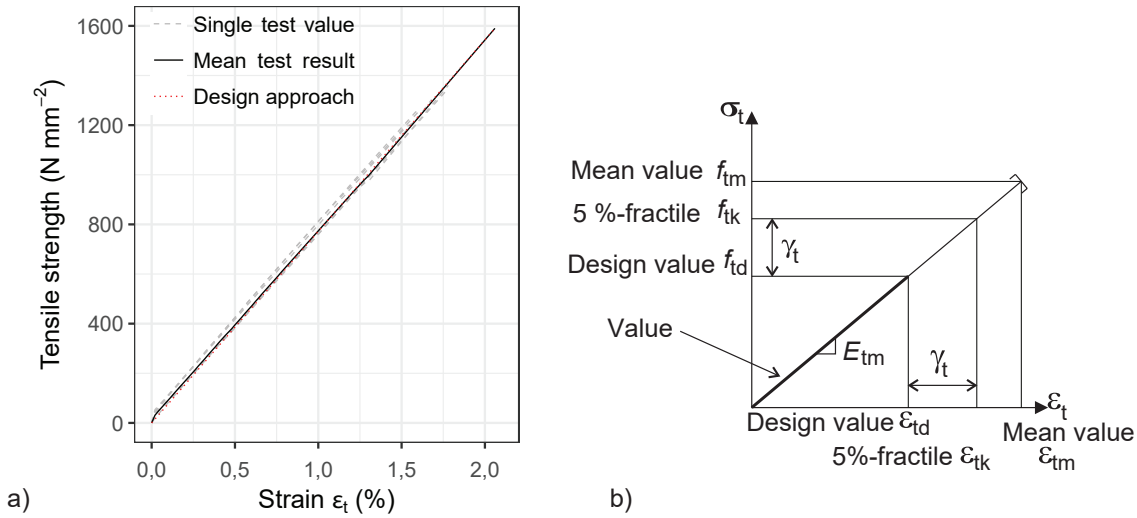

FIGURE 2. Stress-strain diagrams [12](a) AR-glass reinforcement. (b) Design of textile-reinforced components.

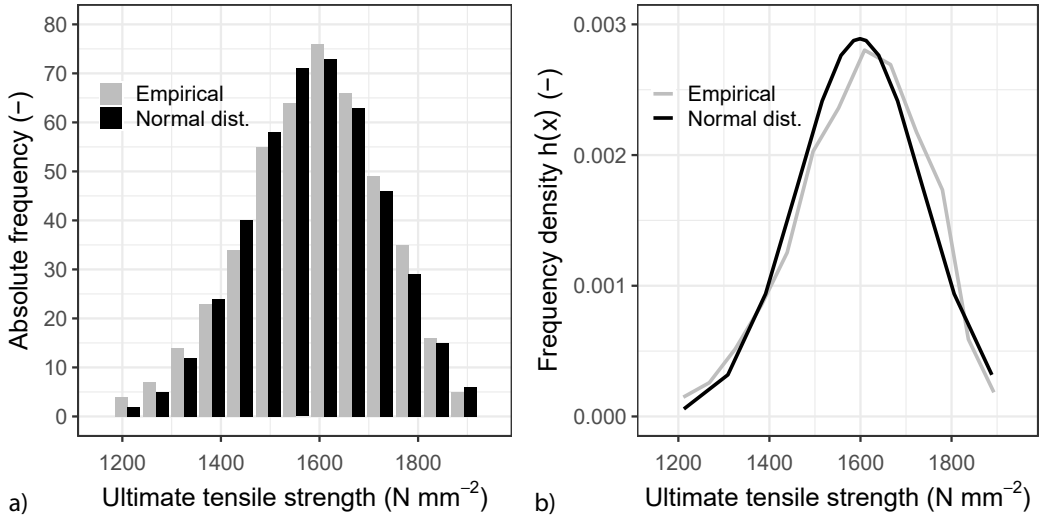

FIGURE 3. Ultimate tensile strength [12]: (a) Histogram for the AR-glass reinforcement (empirical and theoretical values). (b) Probability density function of the AR-glass reinforcement

distribution functions of the material parameters. The test results were used to evaluate the normality assumption, since previous studies assumed that ultimate tensile strengths follow a Normal distribution [22],

The measured ultimate tensile strengths were divided into 13 classes (each with a width of 57 N mm^{-2}) and compiled in a histogram (Figure 3a). The values were then converted into a frequency density $h(x)$ by generating the ratio of the relative frequency to the class width. Through the mean values of each class, a curve of the frequency density was obtained as it is illustrated in Figure 3b. Note that the shape of this curve seems to mirror a Normal distribution. The expected value was approximated by the arithmetic mean value $\mu_X \approx \bar{x}_X = 1\,590$ N mm^{-2} and the standard deviation was estimated by the empirical standard deviation $\sigma_X \approx \bar{s}_X = 138$ N mm^{-2}. These values were considered in the probability density function of a Normal distribution (see Equation 3) [23].

$$f(x) = \frac{1}{138 \cdot \sqrt{2\,\pi}} \exp\left(-\frac{(x - 1\,590}{2 \cdot (138)^2}\right) \qquad (3)$$

To evaluate the data normality, a goodness-of-fit test shall be adopted due to the fact that a single analysis of the graphical plot is not sufficient to confirm that the ultimate tensile strength follows a Normal distribution To this, a *Chi-Square* test was applied, which did not reject normality (i.e., the p-value of 0.70 is above the significance level of 0.05); the arithmetic mean value and the empirical standard deviation were used to approximate the Normal distribution.

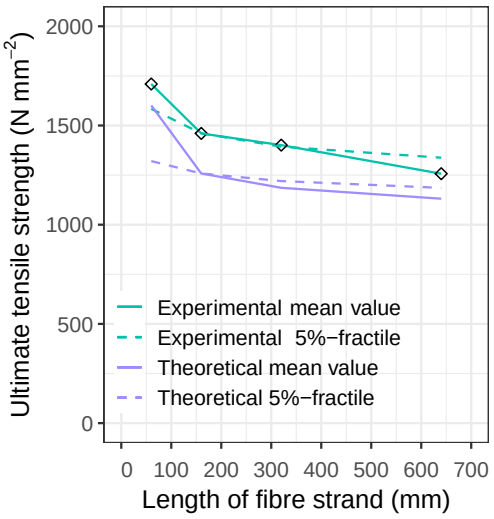

Figure 4. Ultimate tensile strength of the textiles depending on fibre strand length.

3. Investigation of the influence of fibre strand length

3.1. Ultimate tensile strength: experimental investigations

The influence of the fibre strand length on the ultimate tensile strength was investigated for the four lengths of the AR-glass textile placed in the weft direction (i.e., axial direction of the weft strands). At least seven samples were used to test each fibre length. A Normal distribution was assumed to analyse the results. Figure 4 shows the influence of the fibre strand length strand length on the ultimate tensile strength. The mean value decreases with a growing fibre strand length in a non-linear fashion. It is also visible that the mean ultimate tensile strength ranges between 1 709 N mm^{-2} (length = 60 mm) and 1 257 N mm^{-2} (length = 640 mm). The scale effect, which was previously investigated by Griffith [24], can explain such differences, owing to the fact that number of imperfections rises with a growing length of the strand. More recently, Bažant ZP (e.g., [25–27]) carried on extensive studies on the size effects. Also Chudoba [28] and Rypl [29] concluded that the standard deviation is reduced when the strands have an increased length.

3.2. Modulus of elasticity: experimental investigation

For the modulus of elasticity, the influence of the strand length was investigated for the four lengths of the AR-glass textile placed in the weft direction (i.e., axial direction of the weft strands). Also here, at least seven samples were used to test each fibre length. Likewise, a Normal distribution assumption was considered for the modulus of elasticity. Similarly to the ultimate tensile strength, the frequency density curve obtained mirrors a probability density function of a Normal distribution. In this curve, the expected value was approximated by the arithmetic mean value $\mu_X \approx \bar{x}_X = 74\,618$ N mm^{-2} and the standard deviation was determined by the empirical standard deviation $\sigma_X \approx \bar{s}_X = 1\,610$ N mm^{-2}. In the distribution fitting analysis, the *Chi-Square* test did not reject the normality assumption (i.e., p-value of 0.07 is above the significance level of 0.05).

These values seem to confirm that the modulus of elasticity of fibre strands soaked with epoxy resin can be characterised by a Normal distribution function indicating that the statistical parameters can be characterised with the arithmetic mean value and the empirical standard deviation. The entire set of results are available in [14] and in [20].

3.3. Ultimate tensile strength: theoretical investigations

This section addresses the estimation of the statistical parameters for any number of strands, n, using the parameters determined from the experimental tests and extreme value theory.

To this analysis, it was considered that the strands are linked in series. Note that in a series system, the weakest link governs the failure. Furthermore, it was considered that a normally distributed random variable X describes the ultimate tensile strength of each strand.

The calculation of the expected value and the standard deviation of the ultimate tensile strength of a single fibre strand can be conducted with the support of extreme value theory. This theory also supports the distribution function of multiple fibre strands connected in series. Thus, the distribution of the minimum ultimate tensile strength (i.e., governing the series system) – the minimum M_n – can be also determined with the extreme value theory. The distribution function of the minimum $F_{M_n}(x)$ expressed by Equation 4 [30] can be applied to any number of fibre strands n. The results of the standardised tensile tests on fibre strands with a length of 160 mm support the derivation of the cumulative distribution function $F_X(x)$ of the ultimate tensile strength.

$$P(M_n \leq x) = F_{M_n}(x) = 1 - [1 - F_X(x)]^n \quad (4)$$

Equation 4 is only valid for independent and identically distributed random variables with a cumulative distribution function $F_X(x)$ [23]. All the strands linked in series have the same distribution function. By derivating Equation 4, the probability density function $f_{M_n}(x)$ of the minimum ultimate tensile strength M_n can be calculated. Equation 5) allows to determine the probability densities of the extreme value distributions for different lengths.

$$f_{M_n}(x) = f_X(x) \cdot n \cdot [1 - F_X(x)]^{n-1} \quad (5)$$

By rearranging Equation 4, the fractiles of the extreme value distribution can be determined:

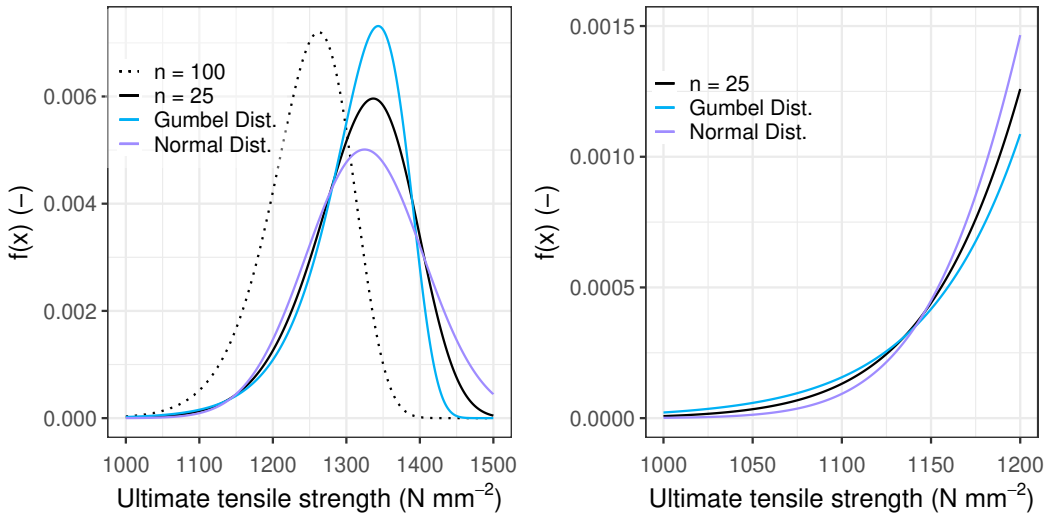

FIGURE 5. Probability density function of the extreme-value function and approximation with Normal and Gumbel distribution functions [20]: (a) entire distribution and (b) selected area of the distribution at the tails.

$$F_{M_n}(x_p) = 1 - [1 - F_X(x_p)]^n = p \tag{6}$$

$$F_X(x_p) = 1 - \sqrt[n]{1-p} \tag{7}$$

Equation 8 can be used to determine the fractile values of the extreme value distribution if the tensile strength of each link is to be normally distributed:

$$x_p = F_X^{-1}(x_p) = \mu_X + \sigma_X \cdot \Phi^{-1}(1 - \sqrt[n]{1-p}) \tag{8}$$

Through Equation 5) it is visible that, as the fibre length increases, the expected value and the standard deviation of the extreme value distribution decrease. Since the density does not present the characteristics of a Normal distribution, a Gumbel distribution (i.e., Generalised Extreme Value distribution, Type-I) [30] was assumed. This distribution can be easily considered in the calculations of reliability analysis when evaluating of the safety level of structural components or systems. A Gumbel distribution is typically characterised by two parameters: a and u and the probability density function (for data minimum) (see Equation 9):

$$f(x) = a \cdot e^{a\cdot(x-u) - e^{a\cdot(x-u)}} \tag{9}$$

The ultimate tensile strengths of the 50%-fractile (median) and the 5%-fractile of the extreme value distribution are calculated to approximate the extreme value distribution by a Gumbel distribution through Equation 5. Then, by using a Gumbel distribution, these fractiles are assumed for the 50%-fractile and the 5%-fractile respectively. Consequently, the parameters a and u of the Gumbel distribution can be calculated.

For two different theoretical values of fibre strands n ($n = 25$ and $n = 100$), the probability density functions of the extreme value distribution were determined

Values of x	Extr. value dist.	Normal dist.	Gumbel dist.
1 194	0.0011180	0.0012952	0.0009687
1 155	0.0004917	0.0005132	0.0004586
1 128	0.0002604	0.0002322	0.0002688
1 046	0.0000302	0.0000107	0.0000534
974	0.0000034	0.0000003	0.0000128

The values of x correspond to the 5%, 2%, 1%, 0.1%, and 0.01% values of the original extreme value distribution.

TABLE 1. Extreme value distribution approximated by a Normal distribution and a Gumbel distribution for $n = 25$ fibre strands [20].

(Figure 5a). It is perceived that the activation of more than 100 fibre strands under a load is highly unlikely. Both distributions – the Normal and the Gumbel – were used to determine the probability density function for each n.

It is widely acknowledged that the behaviour of the distributions at the tails of the functions is of major importance (Figure 5b). By observing the results for $n = 25$, it is visible that an approximation by a Normal distribution sits slightly below the curve of the extreme value distribution. Table 1 shows that for fractile values smaller than 2%, the Gumbel distribution is somewhat above the extreme value distribution, whereas the Normal distribution presents lower values. Figure 5b shows that the Normal distribution curve changes its course to below the extreme value distribution curve at an ultimate tensile strength (i.e., roughly below 1 150 N mm^{-2}). Note that Normal distributions are characterised by thinner tails than extreme value distributions tails. Based on these results, it can be argued that a Normal distribution can generate underestimated failure probabilities, which can seriously affect the robustness of reliability analyses. Contrary

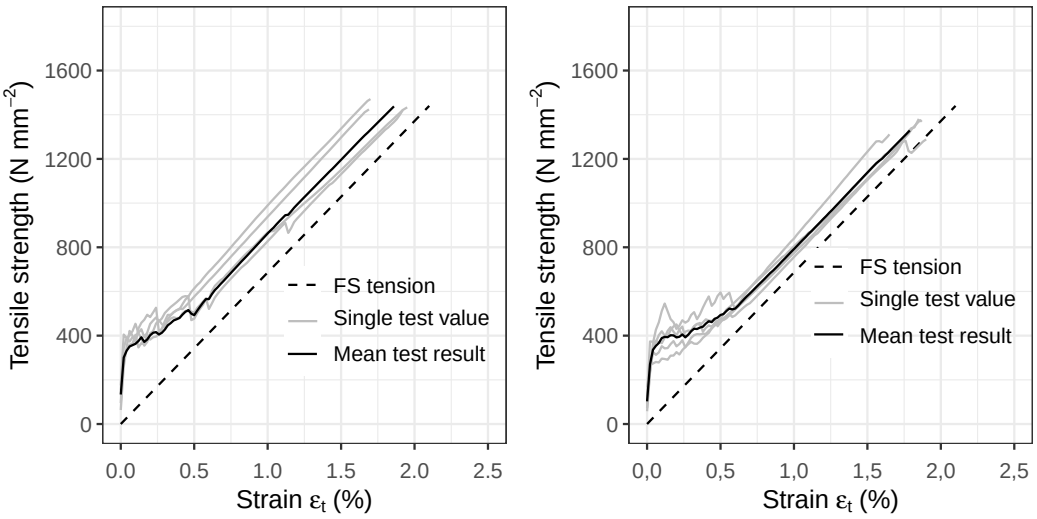

Figure 6. Tension-Strain diagram [12]: a) two and b) eight embedded fibre strands.

to this, a Gumbel distribution seems to be more on the safe side for the assessment of very low failure probabilities.

It is widely recognised that in structural design, the 5%-fractile is a governing value [31, 32], which is also used as the characteristic tensile strength of the textile reinforcement $f_{t,k}$. The design value of the tensile strength $f_{t,d}$ is calculated by dividing the characteristic value $f_{t,k}$ by the partial safety factor γ_t. By assuming a partial safety factor γ_t=1.0, the characteristic value would be equal to the design value.

4. Investigation of the influence of fibre strand number

4.1. Ultimate tensile strength: experimental investigations

In this section, the influence of the number of fibre strands on the ultimate tensile strength is investigated. To this, uniaxial tensile tests on composite members (i.e., textile embedded in the concrete matrix) were used. The results of 40 tests (i.e., eight series with five tests each, beginning with one fibre strand and ending with eight) were considered. The fibre strand tension (i.e., FS tension) of the strands (i.e., tension at the strand without concrete) are represented in Figures 6a and 6b alongside the mean and the single test results.

Equation 1 was used to determine the textile tension σ_t by means of the measured force F and the accumulated filament cross sectional area A_r.

Figures 6 and 6b show that a textile failure always occurs in the tensile tests of the composite members. The black curve shows the mean course of the individual experiments and the grey curve shows the results of the individual experiments. In Figure 6a it is also visible that three cracking states: state I (uncracked), state IIa (crack formation) and state IIb (stabilised crack phase). In state IIb, the curve does not flatten, but runs parallel to the results of the standardised tensile test on the plain fibre strand, which is illustrated as dashed lines. In both tests, the same modulus of elasticity for the textile is achieved in state IIb. This behaviour leads to believe that the results of the test setup can be used to assess the influence of the number of fibre strands. Additionally, the number of fibre strands do not seem to affect the modulus of elasticity.

4.2. Ultimate tensile strength: theoretical investigations

A mathematical relationship for any number of fibre strands can be determined by assuming that fibre strands with the length of 160 mm are theoretically and successively connected next to one another. Here, each element follows a Normal distribution, which was determined with the standardised tensile test for a single strand. Note that here, a brittle failure occurs as soon as the end of the linear-elastic range is reached as opposed to steel that follows a ductile failure behaviour. Each fibre strand in the system is loaded with the same load during the testing procedures. Yet, the strands have distinct ultimate tensile strengths as a result of the material variation. When the ultimate tensile strength of the weakest element is reached, it suddenly fails, and the force is absorbed by the remaining elements. A redistribution can only take place if the remaining fibre strands have sufficient residual load-bearing capacity, which is only possible with a high number of fibre strands, or a large variation of the ultimate tensile strength. Considering a system with n identical fibre strands, which ultimate tensile strengths X_i follow a cumulative distribution function $F_X(\mathrm{x})$, the ultimate tensile strength R can be described as [33]:

$$R = \max(n \cdot \hat{X}_1, (n-1) \cdot \hat{X}_2, ..., \hat{X}_n) \qquad (10)$$

with $\hat{X}_1$, ..., $\hat{X}_n$ being the ultimate tensile strength of the individual strand sorted in ascending order by

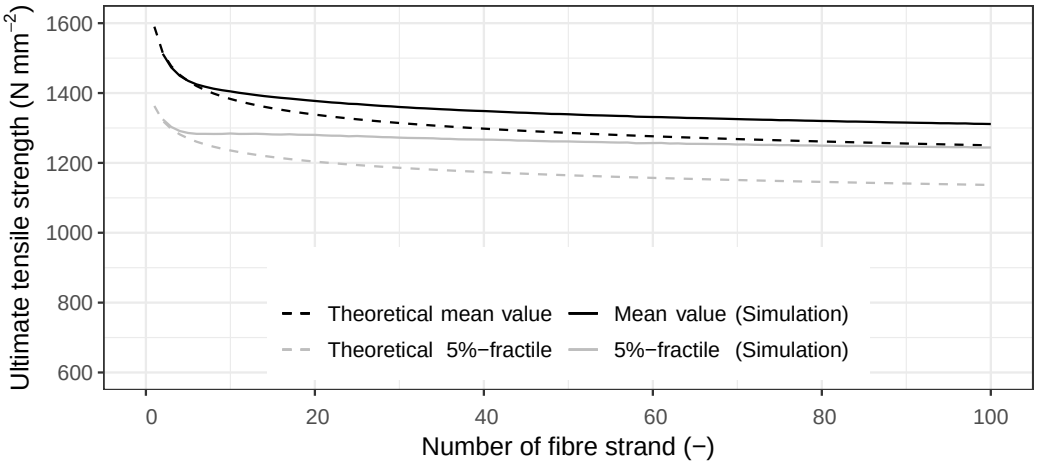

FIGURE 7. Influence of the fibre strand number on the ultimate tensile strength [20].

No. fibre strands	Expected value (i.e., mean value) N mm^{-2}			5%-fractile value N mm^{-2}		
	Simulation	Gumbel dist.	Diff. (%)	Simulation	Gumbel dist.	Diff. (%)
5	1 435	1 434	-0.07	1 281	1 270	-0.87
10	1 404	1 383	-1.55	1 282	1 236	-3.71
25	1 367	1 325	-3.21	1 272	1 194	-6.57
50	1 339	1 286	-4.13	1 258	1 165	-7.96
75	1 323	1 265	-4.55	1 247	1 148	-8.63
100	1 311	1 250	-4.90	1 241	1 137	-9.10

TABLE 2. Ultimate tensile strength: Differences between simulated and theoretical values [20].

size. It can be argued that a safe approximation can be made by assuming that the weakest link governs the failure mechanism. Thus, a parallel connection can be compared to the behaviour of a series connection due to the nearly ideal brittle behaviour of the components. Consequently, Equation 4 can be used to determine the cumulative distribution function of the minima $F_{M_n}(x)$.

4.3. Trade-off between experimental and theoretical investigations

In this section, the experimental and theoretical investigations are compared. To this, a chain system of fibre strands was considered. A Gumbel distribution was assumed to calculate the theoretical mean value and the characteristic value of the ultimate tensile strengths (5%-fractile). These values were used to characterise the ultimate tensile strength, where the mean value is $\mu_X \approx \bar{x}_X = 1\,590$ N mm^{-2} and the empirical standard deviation is $\sigma_X \approx \bar{s}_X = 138$ N mm^{-2}.

Simultaneously, 50 000 simulations were performed in the statistical software *R* [34] by using the principles of Crude Monte-Carlo. Here, it was considered that when the weakest fibre strand fails and the stresses are redistributed to the remaining fibre strands of the system. Additionally, a theoretical expected value was determined by means of Equation 7 (see Figure 7 and Table 2).

The results of the simulation seem to indicate that as the number of fibre strands rises, the average ultimate tensile strength decreases. At some point, the curves tend to flatten. Consequently, the standard deviation and the coefficient of variation also decrease with an increasing number of fibre strands. The extreme value distribution approximated by a Gumbel distribution loses expression (i.e., decreases at a very slow pace) for a growing number of fibre strands. The results in table Table 2 indicate that the differences between the simulated values and the mathematical approximation through a Gumbel distribution can go up to around 9%. A possible explanation is linked to the fact that the Gumbel distribution does not consider a redistribution of stresses after the failure of the first fibre strand. Thus, a Gumbel approximation seems to be on the safe side.

4.4. Practical implications

As described in [17, 35–37], the design value of the tensile strength f_{td} is the basis for the structural calculations with bending and shear load. Yet, a conversion must be made to enable the use of the standardised test results in general structural applications.

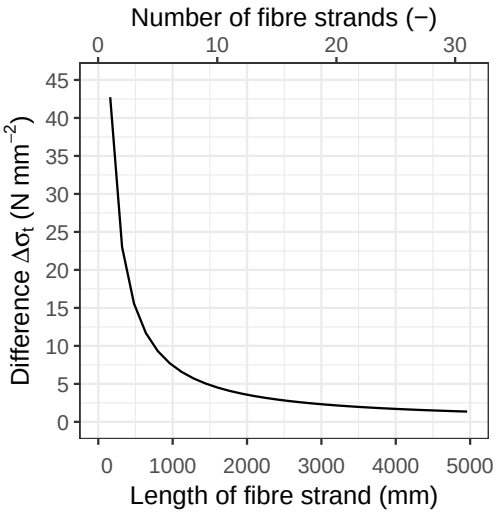

Figure 8. Differences between the n and n-1 fibre strands (5%-fractile values) [12].

This can be achieved by using the 5%-fractile values; note that the characteristic tensile strength of the reinforcement f_{tk} form the basis for the design values of the tensile strength f_{td}. Since the 5%-fractile needs to be used for the design, the problem is not as pronounced, as it can be seen in Figure 8, where the different lengths and numbers of fibre strands are illustrated. The difference is generated from the 5%-fractile values of the ultimate tensile strength of n and $(n-1)$ fibre strands.

For a small number of fibre strands, the 5%-fractile of the tensile strength is influenced by the number of fibre strands (Figure 8). From around five strands, the curve tends to rapidly flatten and the difference between the characteristic values becomes gradually smaller. The gradient is almost constant from a length of 1 600 mm (i.e., around ten strands). In the case of the analysed AR-glass, the value is 4.5 $\mathrm{N\,mm^{-2}}$, which corresponds to just 2.8‰ of the mean ultimate tensile strength. Thus, a reasonable number of fibre strands is suggested for the calculation of the characteristic value. This corresponds to the area where the curve slope of the 5%-fractile becomes almost constant. Yet, a specific number of strands varies with the practical problem. The standardised tensile test needs to be carried out on an individual fibre strand, and then, the ultimate tensile strength must be adjusted by using the extreme value theory. With this approximation, the mean value f_{tm}, the characteristic value f_{tk} , and finally, the design value f_{td} can be determined.

The design strain ε_{td} is also required for the design model. It is sufficient to measure the textile tension and divide it by the modulus of elasticity. The tests showed that the modulus of elasticity is not influenced by the number of fibre strands. The mean value from the standardised test on a single fibre strand can be used as an appropriate modulus of elasticity.

5. Conclusion

In this paper it was demonstrated that the results of a standardised tensile test can be used to derive the statistical values of relevant textile reinforcement properties. This is particularly relevant for the design of components with textile reinforcement impregnated with epoxy resin. By using a reference strand length of 160 mm in the standardised tensile test, only the measurements of the ultimate tensile strength and the modulus of elasticity of a fibre strand are needed.

The test results showed that a fibre strand has a linear-elastic behaviour until it fails when subjected to tensile stress. The length and number of fibre strands seem to influence the ultimate tensile strength. The expected value and the scatter of the ultimate tensile strength decrease non-linearly with a growing length and number of fibre strands. Yet, once a certain fibre length and number is exceeded, the characteristic ultimate tensile strength are no longer affected. In this investigation, it was demonstrated that the statistical values can be determined for any length and number of strands by using the extreme value theory. In this context, calculations are simplified because an extreme value distribution can be approximated by a Gumbel distribution. For the modulus of elasticity, the use of a Normal distribution is recommended.

Acknowledgements

The authors thank the two companies: Solidian GmbH and FTA-Forschungsgesellschaft für Textiltechnik Albstadt GmbH for their support in carrying out the fibre strand tensile tests and providing the textile reinforcements.

References

[1] S. Rempel, N. Will, J. Hegger, P. Beul. Filigrane Bauwerke aus Textilbeton: Leistungsfähigkeit und Anwendungspotenzial des innovativen Verbundwerkstoffs. *Beton-und Stahlbetonbau* **110**(S1):83–93, 2015. https://doi.org/10.1002/best.201400111.

[2] V. Adam, J. Bielak, C. Dommes, et al. Flexural and shear tests on reinforced concrete bridge deck slab segments with a textile-reinforced concrete strengthening layer. *Materials* **13**(18):4210, 2020. https://doi.org/10.3390/ma13184210.

[3] J. Bielak, M. Schmidt, J. Hegger, F. Jesse. Structural behavior of large-scale I-Beams with combined textile and CFRP reinforcement. *Applied Sciences* **10**(13):4625, 2020. https://doi.org/10.3390/app10134625.

[4] J. Bielak, N. Will, J. Hegger. Zwei Praxisbeispiele zur Querkrafttragfähigkeit von Brückenplatten aus Textilbeton. *Bautechnik* **97**(7):499–507, 2020. https://doi.org/10.1002/bate.202000037.

[5] V. Adam, J. Bielak, N. Will, J. Hegger. Experimentelle Untersuchungen zur Verstärkung von Brückenfahrbahnplatten mit Textilbeton. *Beton-und Stahlbetonbau* **115**(12):952–961, 2020. https://doi.org/10.1002/best.202000049.

[6] A. Spelter, S. Bergmann, J. Bielak, J. Hegger. Long-term durability of carbon-reinforced concrete: An overview and experimental investigations. *Applied*

Sciences **9**(8):1651, 2019. https://doi.org/10.3390/app9081651.

[7] A. Spelter, S. Rempel, N. Will, J. Hegger. Prüfkonzept zur Untersuchung des Dauerstandverhaltens von textilbewehrtem Beton. *Bauingenieur* **92**(9), 2017. https://doi.org/10.37544/0005-6650-2017-09-48.

[8] A. Spelter, S. Rempel, N. Will, J. Hegger. Testing concept for the investigation of the long-term durability of textile reinforced concrete. *Special Publication* **326**:55–1, 2018. https://doi.org/10.14359/51711038.

[9] J. Wagner, A. Spelter, J. Hegger, M. Curbach. Ermüdungsverhalten von Carbonbeton unter Zugschwellbelastung. *Beton-und Stahlbetonbau* **115**(9):710–719, 2020. https://doi.org/10.1002/best.201900104.

[10] T. Helbig, K. Unterer, C. Kulas, et al. Fuß- und Radwegbrücke aus Carbonbeton in Albstadt-Ebingen: Die weltweit erste ausschließlich carbonfaserbewehrte Betonbrücke. *Beton-und Stahlbetonbau* **111**(10):676–685, 2016. https://doi.org/10.1002/best.201600058.

[11] M. Hinzen. Prüfmethode zur Ermittlung des Zugtragverhaltens von textiler Bewehrung für Beton. *Bauingenieur* **92**(6):289–291, 2017. https://doi.org/10.37544/0005-6650-2017-06-85.

[12] S. Rempel, M. Ricker. Ermittlung der Materialkennwerte der Bewehrung für die Bemessung von textilbewehrten Bauteilen. *Bauingenieur* **92**(6), 2017. https://doi.org/10.37544/0005-6650-2017-06-76.

[13] R. Alex. Fibre reinforced polymers FRP as reinforcement for concrete according to German approvals. In *IOP Conference Series: Materials Science and Engineering*, vol. 96, p. 012013. IOP Publishing, 2015. https://doi.org/10.1088/1757-899x/96/1/012013.

[14] S. Rempel, M. Ricker, J. Hegger. Zur Zuverlässigkeit der Bemessung von biegebeanspruchten Betonbauteilen mit textiler Bewehrung. Tech. rep., Lehrstuhl und Institut für Massivbau, 2019.

[15] S. Voss. *Ingenieurmodelle zum Tragverhalten von Textilbewehrtem Beton*. Eigenverlag, Lehrstuhl und Institut für Massivbau der RWTH Aachen, 2008.

[16] M. Ricker, T. Feiri, K. Nille-Hauf, et al. Enhanced reliability assessment of punching shear resistance models for flat slabs without shear reinforcement. *Engineering Structures* **226**:111319, 2021. https://doi.org/10.1016/j.engstruct.2020.111319.

[17] S. Rempel, M. Ricker, J. Hegger. Safety concept for textile-reinforced concrete structures with bending load. *Applied Sciences* **10**(20):7328, 2020. https://doi.org/10.3390/app10207328.

[18] E. M. Silva, S. E. Ribeiro, S. Diniz. Reliability-based design recommendations for deflection control of fiber-reinforced polymer-reinforced concrete beams. *ACI Structural Journal* **117**(3), 2020. https://doi.org/10.14359/51723499.

[19] R. Moceikis, A. Kičaitė, G. Skripkiūnas, A. Korjakins. Ageing models and accelerated ageing tests of glass fiber reinforced concrete. *Engineering Structures and Technologies* **10**(1):10–17, 2018. https://doi.org/10.3846/est.2018.1467.

[20] S. Rempel, M. Ricker, T. Feiri. Stochastic approach for the material properties of reinforcing textiles for the design of concrete members. *Scientific Reports* **11**(1):2045–2322, 2021. https://doi.org/10.1038/s41598-021-01032-9.

[21] W. Brameshuber, M. Hinzen, A. Dubey, et al. Recommendation of RILEM TC 232-TDT: Test methods and design of textile reinforced concrete: Uniaxial tensile test: test method to determine the load bearing behavior of tensile specimens made of textile reinforced concrete. *Materials and Structures/Materiaux et Constructions* **49**(12):4923–4927, 2016. https://doi.org/10.1617/s11527-016-0839-z.

[22] C. Kulas. Zum Tragverhalten getränkter textiler Bewehrungselemente für Betonbauteile. Tech. rep., Lehrstuhl und Institut für Massivbau, 2013.

[23] M. Holickỳ. *Introduction to probability and statistics for engineers*. Springer Science & Business Media, 2013.

[24] A. Griffith. VI. The phenomena of rupture and flow in solids. *Philosophical transactions of the Royal Society of London Series A, containing papers of a mathematical or physical character* **221**(582-593):163–198, 1921. https://doi.org/10.1098/rsta.1921.0006.

[25] Z. P. Bažant. Size effect in blunt fracture: concrete, rock, metal. *Journal of engineering mechanics* **110**(4):518–535, 1984. https://doi.org/10.1061/(asce)0733-9399(1984)110:4(518).

[26] Z. P. Bažant, J. Planas. *Fracture and size effect in concrete and other quasibrittle materials*, vol. 16. CRC press, 1997. https://doi.org/10.1201/9780203756799.

[27] Z. P. Bažant. Size effect. *International Journal of Solids and Structures* **37**(1-2):69–80, 2000. https://doi.org/0.1016/S0020-7683(99)00077-3.

[28] R. Chudoba, M. Vořechovskỳ, V. Eckers, T. Gries. Effect of twist, fineness, loading rate and length on tensile behavior of multifilament yarns (a multivariate study). *Textile Research Journal* **77**(11):880–891, 2007. https://doi.org/10.1177/0040517507081280.

[29] R. Rypl, R. Chudoba, U. Mörschel, et al. A novel tensile test device for effective testing of high-modulus multi-filament yarns. *Journal of Industrial Textiles* **44**(6):934–947, 2015. https://doi.org/10.1177/1528083714521069.

[30] A. Meyna, B. Pauli. Taschenbuch der Zuverlässigkeitstechnik: Quantitative Bewertungsverfahren, 2., überarb. u. erw. *Aufl Hanser, München* 2010.

[31] J. P. M. Code. Joint Committee on Structural Safety. *URL: www jcssethzch* 2001.

[32] Eurocode: Basis of Structural Design. CEN European Committee for Standardization, 2002.

[33] H. E. Daniels. The statistical theory of the strength of bundles of threads. I. *Proceedings of the Royal Society of London Series A Mathematical and Physical Sciences* **183**(995):405–435, 1945. https://doi.org/10.1098/rspa.1945.0011.

[34] R. C. Team, et al. R: A language and environment for statistical computing 2013.

[35] S. Rempel, M. Ricker, J. Hegger. Biegebemessungsmodell mit einer geschlossenen und iterativen Lösung für Textilbetonbauteile: Reine Biegung und Biegung mit Normalkrafteinfluss. *Beton-und Stahlbetonbau* **115**(3):218–230, 2020. https://doi.org/10.1002/best.201900086.

[36] J. Bielak, V. Adam, J. Hegger, M. Classen. Shear capacity of textile-reinforced concrete slabs without shear reinforcement. *Applied Sciences* **9**(7):1382, 2019. https://doi.org/10.3390/app9071382.

[37] J. Bielak, J. Hegger, M. Schmidt. Shear capacity of carbon fibre textile reinforced concrete slabs with planar and C-shaped shear reinforcement. *Proceedings of the Fiber Reinforced Polymer Reinforced Concrete Structures* **14**, 2019.